

Supporting Information

Rate-determining Step Backshift Effectively Boost ORR Performance by excess Electrons transfer to O-O Antibonding orbital

Lili Zhang,^a Shengwei Yu,^b Xiang Xie,^a Jiayi Zeng,^a Hongliang Jiang,^b Jianhua Shen,^a

*Haibo Jiang, ^{*a} Chunzhong Li^{*a}*

a. Shanghai Engineering Research Center of Hierarchical Nanomaterials, Key Laboratory for Ultrafine Materials of Ministry of Education, School of Materials Science and Engineering, East China University of Science & Technology, Shanghai 200237, China. E-mail: czli@ecust.edu.cn;

b. School of Chemical Engineering, East China University of Science and Technology, Shanghai 200237, China. E-mail: yushengwei0036@163.com.

Experimental section

1. Materials and Chemicals:

Platinum (II) acetylacetonate ($\text{Pt}(\text{acac})_2$, $\geq 99\%$), Palladium (II) acetylacetonate ($\text{Pd}(\text{acac})_2$, $\geq 99\%$), Hexadecyltrimethylammonium bromide (CTAB), Anhydrous Glucose ($\text{C}_6\text{H}_{12}\text{O}_6$), Oleamine ($\text{C}_{18}\text{H}_{37}\text{N}$, 70%), oleic acid ($\text{C}_{18}\text{H}_{34}\text{O}_2$) were purchased from Aladdin. 20 wt% Pt/C was purchased from Shanghai Hesen Electric. Vulcan XC-72 was purchased from Macklin. All chemicals were used as received and not further purified. Electrolyte solutions were prepared with deionized water (resistance: 18.2 $\text{M}\Omega$).

2. Synthesis of $\text{Pt}_{23}\text{Pd}_{77}$ NSs

In a typical synthesis of $\text{Pt}_{23}\text{Pd}_{77}$ NSs, 10 mg $\text{Pt}(\text{acac})_2$, 22.8 mg $\text{Pd}(\text{acac})_2$, 60 mg CTAB, and 100 mg glucose were added to a 40 mL transparent glass reaction flask, and then 15 mL of non-precipitated oleamine and 50 μL oleic acid were added to the 40 mL transparent glass reaction flask, and sonicated for about 30 min until a homogeneous dispersion was formed. CO was then introduced into the reaction (flow: 50 mL/min) and held for 15 minutes. The vial was capped and sealed and heated to 200 $^\circ\text{C}$ for 2 h at room temperature. After the reaction, the product was naturally cooled, centrifuged at 10,000 rpm, washed twice with a mixed solution with an ethanol/cyclohexane volume ratio of 3:1 and redispersed in cyclohexane, and the catalyst was named $\text{Pt}_{23}\text{Pd}_{77}$ NSs.

3. Synthesis of Pt_xPd_y NSs and Pt NPs

As a contrast, catalysts of different compositions were obtained by adjusting the ratio of metal precursors. Pt NPs, Pd NSs, $\text{Pt}_{48}\text{Pd}_{52}$ NSs, and $\text{Pt}_{17}\text{Pd}_{83}$ NSs were fed with 10 mg $\text{Pt}(\text{acac})_2$, 7.6 mg $\text{Pd}(\text{acac})_2$, 10 mg $\text{Pt}(\text{acac})_2$, 7.6 mg $\text{Pd}(\text{acac})_2$, 10 mg $\text{Pt}(\text{acac})_2$, 10 mg $\text{Pd}(\text{acac})_2$, and 38 mg $\text{Pd}(\text{acac})_2$, respectively, and other conditions remained unchanged.

4. Characterization

High-angle annular dark field scanning transmission electron microscopy (HAADF-STEM) images and TEM images were taken by the JEOL-2100 experimental setup with LaB6 cathode at 200 kV. High angle annular dark field scanning transmission electron (HAADF-STEM) imaging was performed on a Grand ARM 300F connected to an energy-dispersive X-ray spectroscopy (EDX). Inductively coupled plasma-atomic emission spectroscopy (ICP-AES) was manipulated to assess the concentration of the catalyst on Agilent 725ES. X-ray photoelectron spectroscopy (XPS) measurements were carried out using K-Alpha Plus (Somerfield, USA) with Al-K α X-ray as the illuminant to Obtain the electronic structure and elemental composition of catalyst surfaces. The X-ray diffraction patterns of catalyst particles were collected on a D8 ADVANCE (Bruker, Germany) diffractometer in Cu K α radiation ($\lambda = 1.5406 \text{ \AA}$) to determine the crystal structure and particle size. The operation voltage and current were 40 kV and 20 mA, respectively.

5. Electrochemical tests

Before the electrocatalytic test, the Pt₂₃Pd₇₇ NSs were loaded on carbon supports (Vulcan XC-72) with a 20 wt% loading of total metal (Pt+Pd) (determined by ICP-MS). PtPd NSs were loaded onto the Vulcan XC-72 in the following process: PtPd NSs and carbon carriers were dispersed in ethanol, respectively. These two homogeneous solutions are then mixed together Sonicate for 1 h. The prepared Pt₂₃Pd₇₇ NSs/C catalyst was then collected by centrifugation at 10,000 rpm, washed with ethanol, and dried in a vacuum oven.

All electrochemical measurements were operated in a standard three-electrode system. The glassy carbon electrode was mounted on a rotating disk electrode as the working electrode (5 mm in diameter), a saturated calomel electrode as the reference electrode, and a carbon rod as the counter electrode. The electrode potential was reported with reference to the reversible hydrogen electrode (RHE) by calibrating the

equation $E_{RHE}=E_{SCE}+0.24+0.0591*\text{pH}$. Catalyst ink was obtained by dispersing 2.5 mg of catalyst powder in a mixture of 960 μL of isopropanol and 40 μL of Nafion (5 wt.%) and sonicated for 2 h. The catalyst film was obtained by depositing 4 μL of ultrasonically homogeneous catalyst ink on the glassy carbon electrode and drying naturally at room temperature.

Cyclic voltammetry (CV) curves were recorded in a 0.1 M KOH aqueous solution passed through Ar at least 30 min with a potential interval of 0.01 V-1.31 V (vs RHE) and a scan rate of 100 mV s^{-1} . ORR polarization curves were recorded in 0.1 M KOH solution saturated with O_2 using linear scanning voltammetry (LSV) curves at 1600 rpm and a scan rate of 10 mV s^{-1} . Accelerated durability tests (ADT) were conducted by cycling between 0.6 V and 1.0 V versus RHE at a scanning rate of 100 mV s^{-1} . The ORR performances of the reference samples were also measured through similar procedures.

The electrochemically active surface area (ECSA) is estimated by integrating the area of *OH species reduction peak according to the equation:

$$ECSA = \frac{S/v}{C \times m_{Pt+Pd}}$$

Where S represents the integral area of *OH reduction peak, the m represents mass of catalyst, C is the charge value of hydrogen adsorbed on the Pt surface in the monolayer (210 $\mu\text{C cm}^{-2}$), v is the CV scanning rate. The mass percentage of Pt₂₃Pd₇₇ NSs/C is measured by ICPAES to be 20% with commercial Pt/C of 20.02%. Therefore, the actual loading (m_{PGM}) on the surface of the glassy carbon electrode is 2.0 μg and 4 μg , respectively.

The electrochemically active surface area (ECSA) of Pd-based materials are determined by CO-stripping, assuming a charge density of 420 μC per cm^2 Pt+Pd. The electrode with catalysts was immersed in CO gas (99.999%) saturated 0.1 M HClO_4 to adsorb monolayer CO molecules, then the working electrode was transferred into a fresh Ar-saturated 0.1 M HClO_4 and swept from 0 V to 1.30 V (vs. RHE) at a scan rate

of 20 mV·s⁻¹. The electrochemical surface area of the catalyst is obtained from the following equation:

$$ECSA = \frac{S_{CO}/v}{C \times m_{Pt+Pd}}$$

The ORR kinetic current of the catalyst was obtained by the Koutecky-Levich equation:

$$j_k = \frac{j - j_L}{jj_L}$$

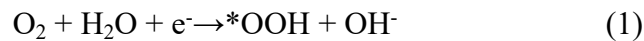
Where j_k is the kinetic current density, j is the measured current density, and j_L is the limiting current density. We took the logarithm of the kinetic current density as the abscissa and the electrode potential as the ordinate to plot the Tafel curve of the reaction, where the slope of the fitted straight line was the Tafel slope.

The number of electron transfers (n) were measured at 400, 900, 1225, 1600, 2025, 2500 rpm, respectively, according to the Koutecky-Levich equation:

$$\frac{1}{j} = \frac{1}{j_L} + \frac{1}{j_k} = \frac{1}{0.62nFC_0D_0^{2/3}v^{-1/6}\omega^{1/2}} + \frac{1}{j_k}$$

Where j is the measured current density, j_k and j_L are the kinetic and diffusion-limiting current densities respectively, ω is the angular velocity, n is transferred electron number, F is Faraday constant (96485 C mol⁻¹), C_0 is the bulk concentration of O₂ (1.2×10⁻⁶ mol cm⁻³), D_0 is the diffusion coefficient of O₂ (1.9×10⁻⁵ cm² s⁻¹), and v is the kinetic viscosity of the electrolyte (0.01 cm² s⁻¹).

Based on the Tafel equation and the ORR reaction mechanism in 0.1 M KOH:



The correspondence between Tafel slope and RDS is based on the Butler-Volmer equation:

$$b = \frac{2.303RT}{\alpha F}$$

where α is the symmetry factor, R, T, and F are the gas constant, temperature, and Faraday constant, respectively. The Tafel equation is an experimental summary, and the experimentally measured Tafel slope b is the apparent value of the multi-step electrochemical reaction, which corresponds to the apparent electron transfer number. Most electrochemical reactions involve multiple electron transfers, so the apparent electron transfer number contains the electron transfer number " α^* " of the RDS and the step electron transfer number n before the RDS, so the Tafel slope should be expressed as:

$$b = \frac{2.303RT}{(\alpha^* + n)F}$$

If the RDS involves 1 electron transfer, $\alpha^* = 0.5$;

Case 1: If there is no electron transfer before RDS, then $n = 0$, $b = 118 \text{ mV dec}^{-1}$, RDS is the first electron transfer, that is $\text{O}_2 + \text{e}^- \rightarrow \text{O}_2^-$.

Case 2: If the number of electron transfers is 1 before RDS, then $n = 1$, $b = 40 \text{ mV dec}^{-1}$, and RDS is the second electron transfer, that is $^*\text{O} + ^*\text{OH} + \text{e}^- \rightarrow ^*\text{O} + \text{OH}^-$.

If the RDS does not involve electron transfer, then $\alpha^* = 0$;

Case 3: If the number of electron transfers is 1 before RDS, then $n = 1$, $b = 60 \text{ mV}$, and RDS is O-O bond, that is $^*\text{OOH} \rightarrow ^*\text{O} + ^*\text{OH}$.

Case 4: If the number of electrons transfers is 2 before RDS, then $n = 2$, $b = 30 \text{ mV}$, and RDS is the subsequent reaction.

The apparent activation energy of the oxygen reduction reaction of the catalyst: First, the electrolyte is poured into the inner layer of the four-port jacketed electrolytic cell, and then we use a constant temperature water bath to feed circulating water into the outer layer of the jacketed electrolytic cell and maintain a specific temperature. The electrolyte temperature is calibrated by a corrected alcohol thermometer. The oxygen reduction reaction polarization curves of the catalyst were obtained at temperatures of

278, 288, 298, 308, and 318 K, respectively. According to the Arrhenius formula and the Butler-Volmer equation:

$$k = A \exp\left(-\frac{E_a}{RT}\right)$$

$$j_k = nFkc$$

Where k is the reaction rate constant, A is the pre-exponential factor, E_a is the apparent activation energy of the reaction, R is the Gas Constant, T is the reaction temperature, j_k is the kinetic current density, n is the number of electrons transferred by the reaction, F is the Faraday Constant, and c is the concentration of the reactant.

$$\ln \frac{j_k}{c_{CO_2}} = -\frac{E_a}{RT} + \ln(nFA)$$

By defining $\frac{j_k}{c_{CO_2}}$ as j'_k at a certain temperature, we can obtain:

$$\ln j'_k = -\frac{E_a}{RT} + \ln(nFA)$$

We can take $1/T$ as the abscissa and $\ln j'_k$ as the ordinate to draw the graph. The slope of the fitted straight line can be obtained and the E_a can be obtained.

The reaction order of OH^- is tested by the following method. Change the KOH concentration to adjust the pH value of the electrolyte and use KCl to ensure that the K^+ concentration remains unchanged. The polarization curve was obtained by linear sweep voltammetry. Take the logarithm of the kinetic current density as the ordinate and the logarithm of OH^- concentration as the abscissa. The slope obtained at different potentials is the OH^- reaction order.

RRDE tests are conducted in a three-electrode system controlled by an electrochemical workstation (CHI760E, CHI1140D, CH Instruments). This system consists of a reference electrode, a counter electrode, and a working electrode. Specifically, Ag/AgCl (RREF0024, Pine Research Instrumentation) is used as the

reference electrode, and graphite is used as the counter electrode. The RRDE included a glassy carbon disk electrode (disk area = 0.2475 cm²) and a Pt ring electrode (ring area = 0.1866cm²) with a theoretical collection efficiency (N) of 0.37. Before conducting electrochemical tests, 0.1 M KOH electrolyte is purged with oxygen for at least 30 minutes. All potentials were calibrated to the RHE reference scale using the formulas as follows:

$$E_{RHE} = E_{Ag/AgCl} + 0.197 + 0.592 * pH$$

Calculate the number of electron transfers (n) and the selectivity of H₂O₂ (%) using the following formulas, where I_r is the circular flow and I_d is the disk flow.

$$H_2O_2(\%) = \frac{200 \times I_r}{|I_d| \times N + I_r}$$

$$n = 4 \times \frac{I_d}{|I_d| + \frac{I_r}{N}}$$

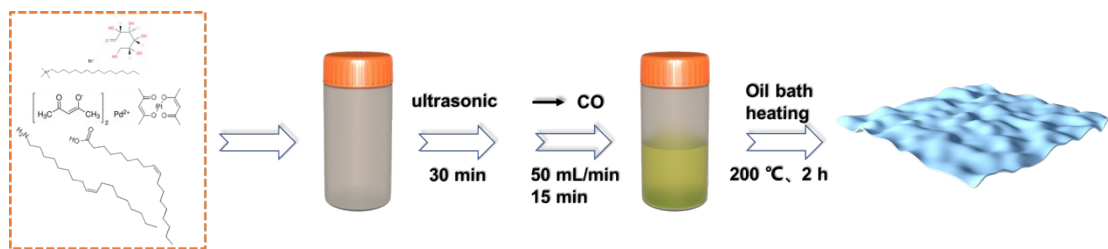
6. Density functional theory method

The first-principles density functional theory (DFT) calculations were performed by the Dmol3 code. The calculation of electronic structure and exchange-correlation effects was based on the generalized gradient approximation and Perdew-Burke-Ernzerh (GGA-PBE) functional. Valence electrons were expanded by the polarization (DNP) function of the dual value basis. The inner electrons were frozen by the semi-nuclear pseudopotential. Based on the high-resolution transmission electron microscopy imaging results, the nanosheet structure was established with pure Pd (110) as the reference, and the PdPt alloy covering two Pd atomic layers was modeled. A four-layer periodic cell was used for simulation, and the bottom two layers periodically replaced Pt atoms with Pd atoms at the ratio of Pt:Pd= 1:3, and then the cell structure was optimized. The bottom two layers of atoms are fixed in place, and the rest of the atoms are relaxed. Then the models went through geometric optimization. The adsorption energies of O (E_{ads}(O)) were calculated via following equation: E_{ads}(O) = E_{total} - E_O - E*, where E_{total}, E_O and E* represented the total energy of adsorption system, the energy of O atom and the energy of adsorption system.

The value of Gibbs free energy change for the oxygen-containing intermediate at a given potential is calculated by the following equation:

$$\Delta G(\text{ad}) = \Delta E(\text{ad}) + \Delta \text{ZPE}(\text{ad}) - T\Delta S(\text{ad}) + (x-4) eU$$

Where $\Delta G(\text{ad})$ is the change of free energy before and after adsorption, $\Delta E(\text{ad})$ is the adsorption energy, $\Delta \text{ZPE}(\text{ad})$ is the zero point energy, $T\Delta S(\text{ad})$ is the effect of entropy change, and x is the total number of electron transfers. Since we considered the adsorption of a monolayer of water in the model, the solvation energy is not considered separately.



Scheme S1. Schematic flow diagram of the preparation of Pd-based nanosheets.

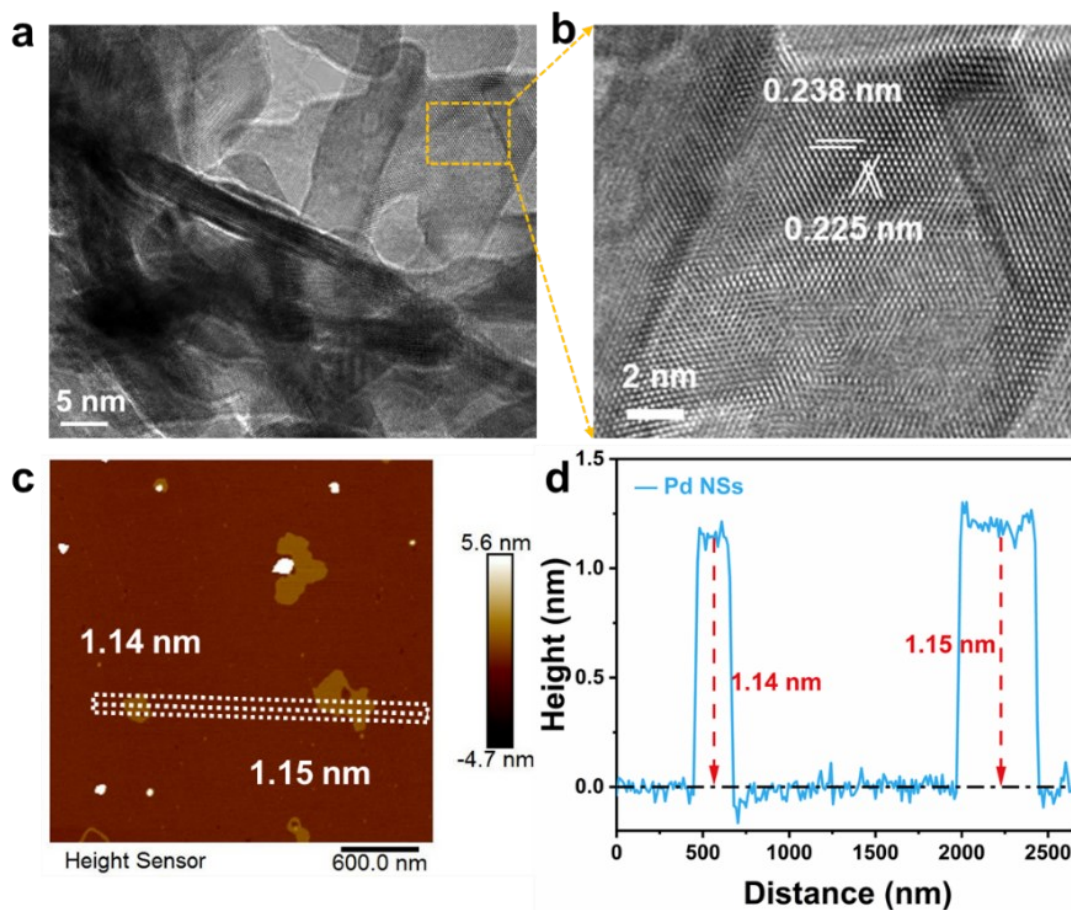


Fig. S1. Morphological and structural characterization of Pd NSs. (a) TEM image. (b) HRTEM image of the yellow rectangular checkbox in (a). (c) Atomic force microscope images. (d) Corresponding height profile of (c).

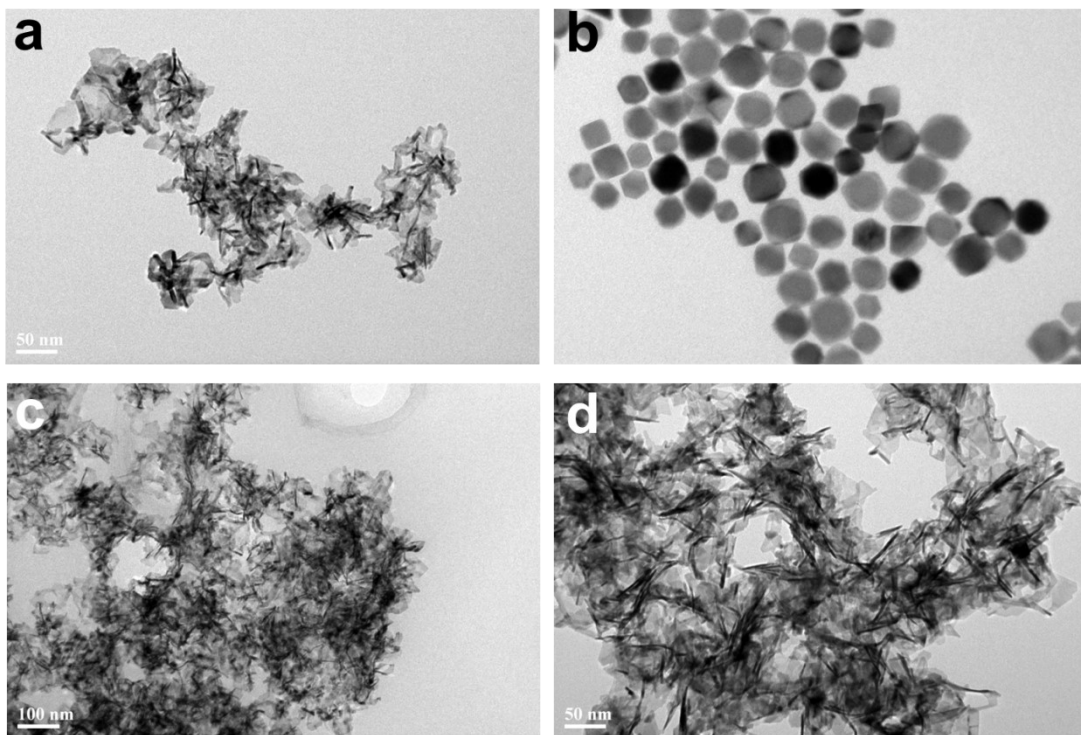


Fig. S2. TEM images and structural characterization of the different components.

(a) Pt₄₈Pd₅₂ NSs. (b) Pt NPs. (c) Pt₁₇Pd₈₃ NSs. (d) Pd NSs.

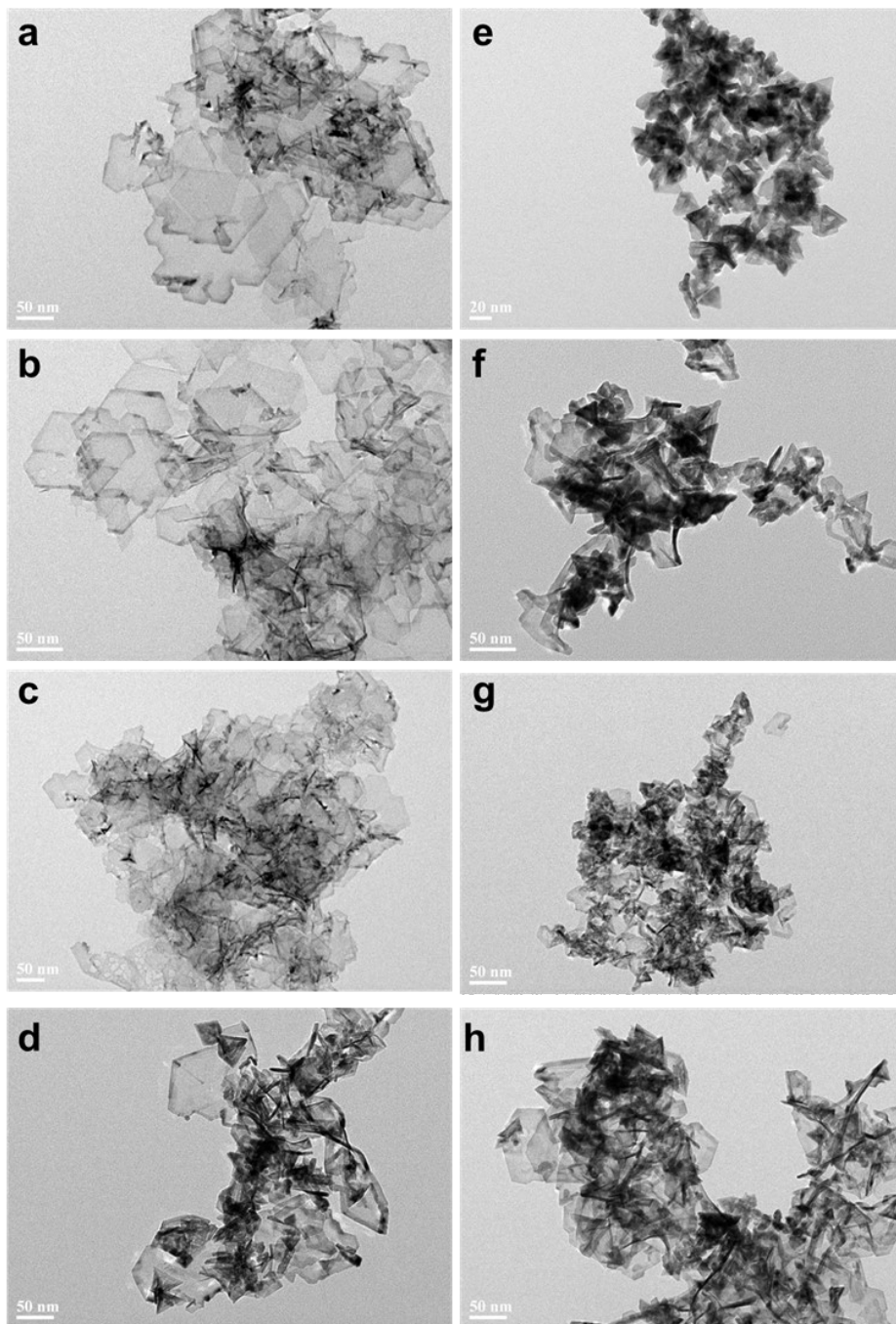


Fig. S3. Structural evolution of $\text{Pt}_{23}\text{Pd}_{77}$ NSs. (a-d) the reaction system keeps the heating time unchanged, and the reaction temperature varies from 80 °C, 120 °C, 160 °C, and 200 °C. (e-h) the reaction system keeps the heating temperature unchanged, and the reaction time varies from 1 min, 10 min, 30 min, and 120 min.

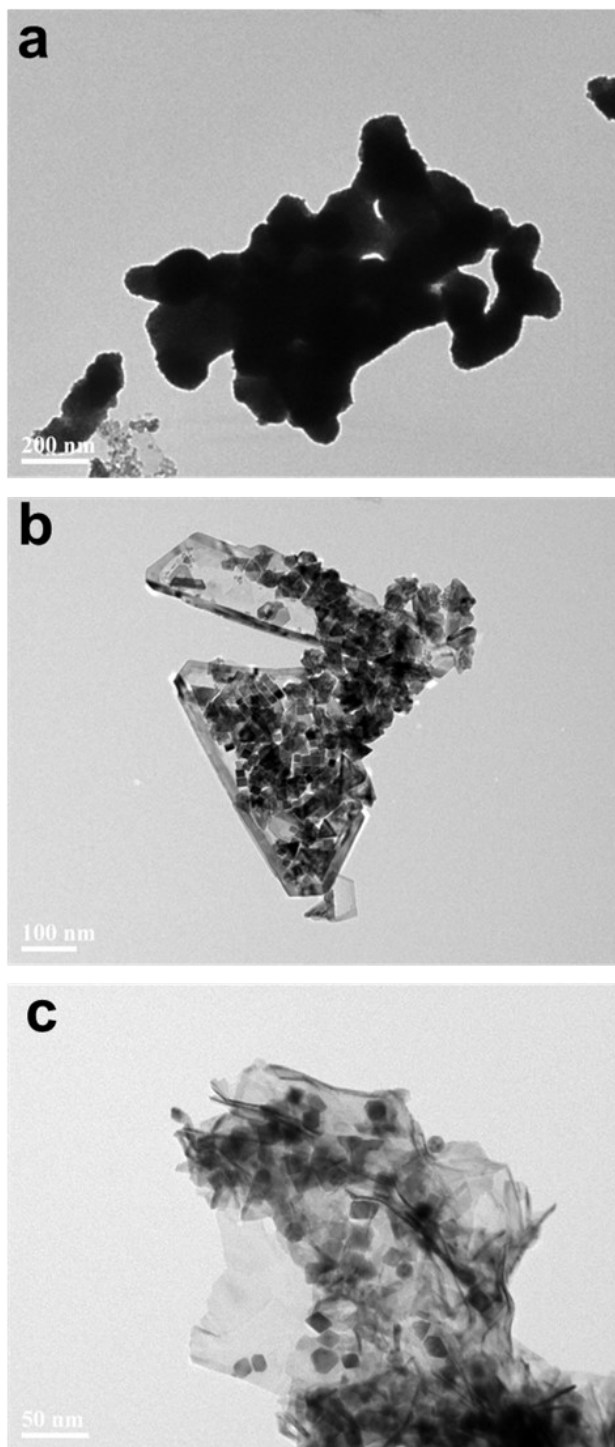


Fig. S4. Effect of surface constraints and capping agents on the shape of $\text{Pt}_{23}\text{Pd}_{77}$ NSs: only one variable was changed, controlling for the same other conditions. (a) no CO was passed. (b) no CTAB was added. (c) CTAB was replaced with NH_4Br .

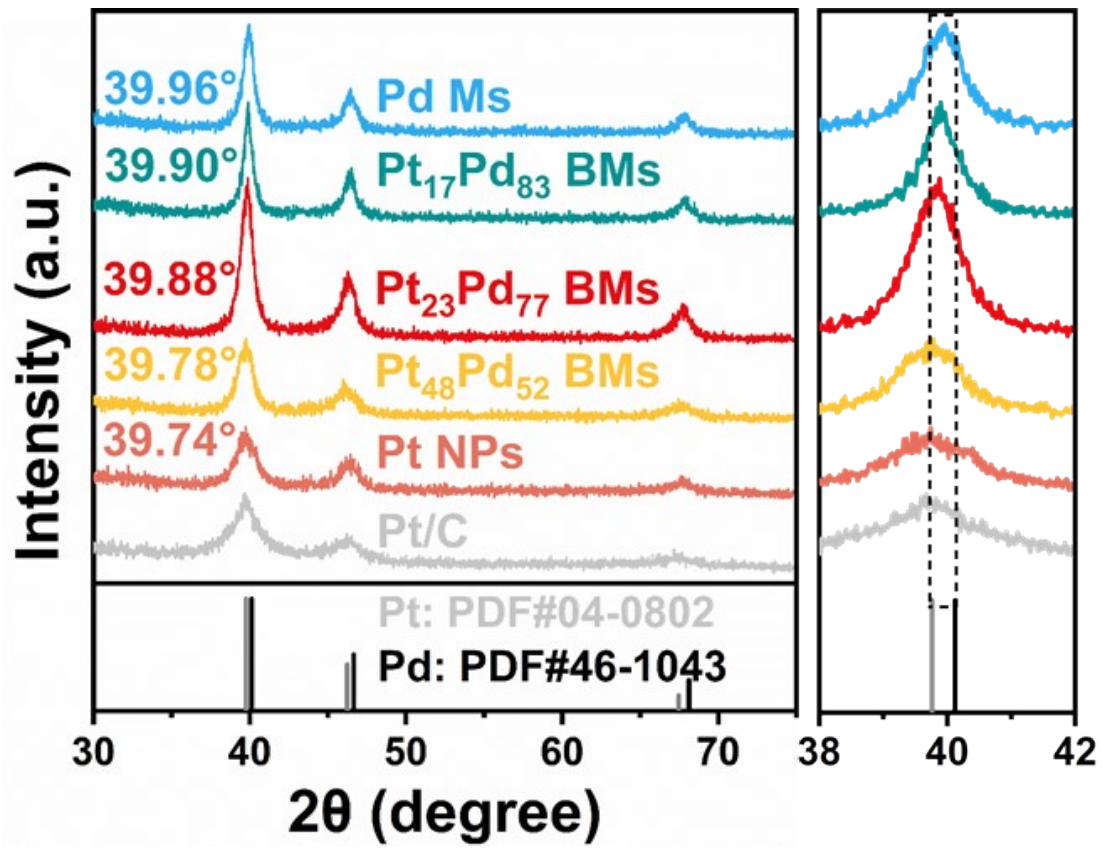


Fig. S5. XRD patterns of each component and magnified patterns of (111) diffraction peak positions

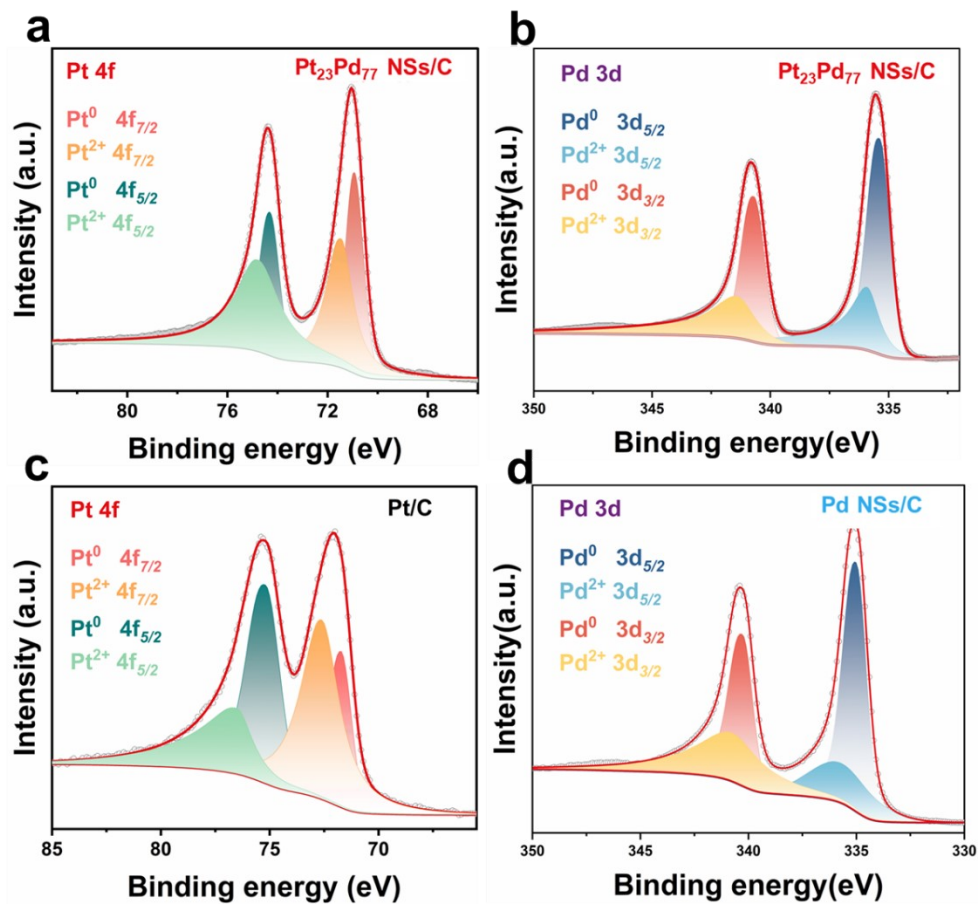


Fig. S6. Corresponding high-resolution XPS spectra. Pt 4f. (a) and Pd 3d. (b) of $Pt_{23}Pd_{77}$ NSs. (c) Pt 4f of Pt/C. (d) Pd 3d of Pd NSs.

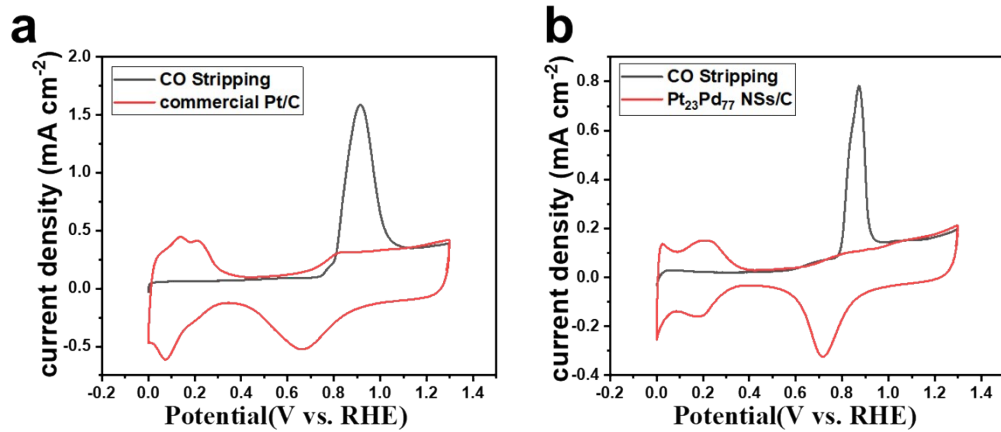


Fig. S7. CO dissolution voltammetry of Pt₂₃Pd₇₇ NSs and commercial Pt/C catalyst. Voltammetry was performed in 0.1 M HClO₄. Scan rate: 20mV s⁻¹. The integrated charge of CO stripping is used to calculate the ECSA of each catalyst. (a)commercial Pt/C. (b)Pt₂₃Pd₇₇ NSs/C.

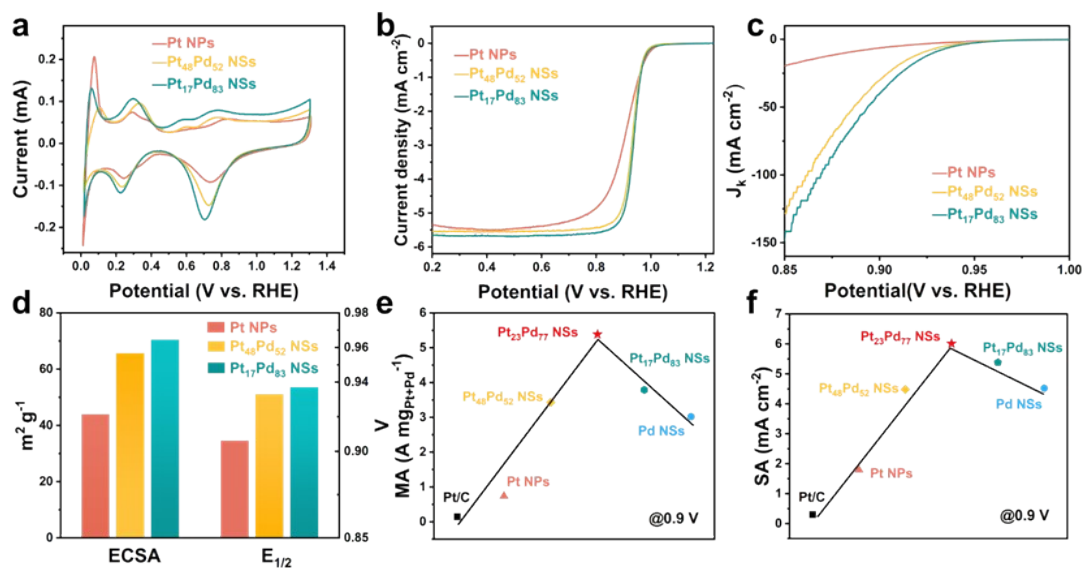


Fig. S8. ORR performance indicators and comparison of Pt NPs, Pt₄₂Pd₅₈ NSs, Pt₁₇Pd₈₃ NSs, and Pt₂₃Pd₇₇ NSs. (a) CV curve. (b) LSV polarization curve. (c) Dynamic current density curve. (d) Comparison of three catalysts ECSA and E_{1/2}. Comparison of mass activity (e) and specific activity (f) at 0.9 V vs. RHE.

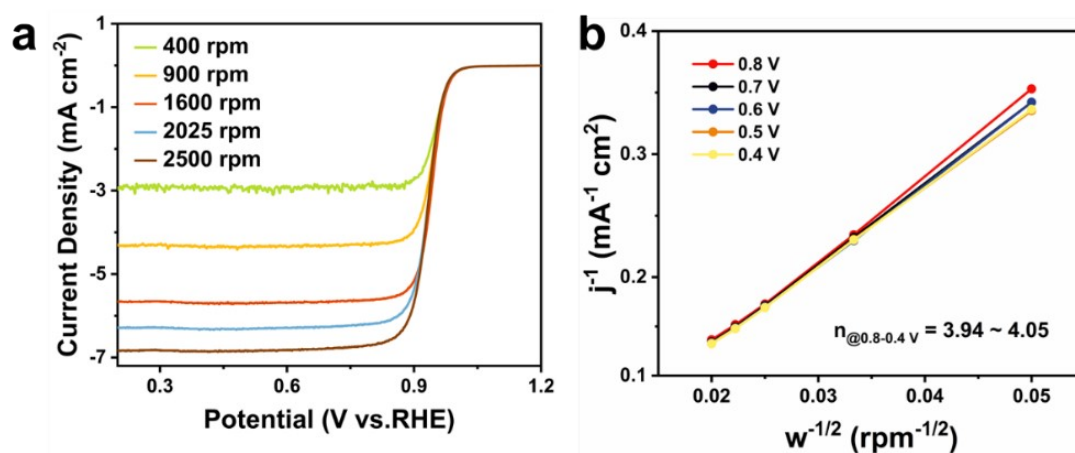


Fig. S9. Determination of electron transfer number of Pt₂₃Pd₇₇ NSs. (a) ORR polarisation curves at different RDE rotation rates. (b) electron transfer number at different potentials.

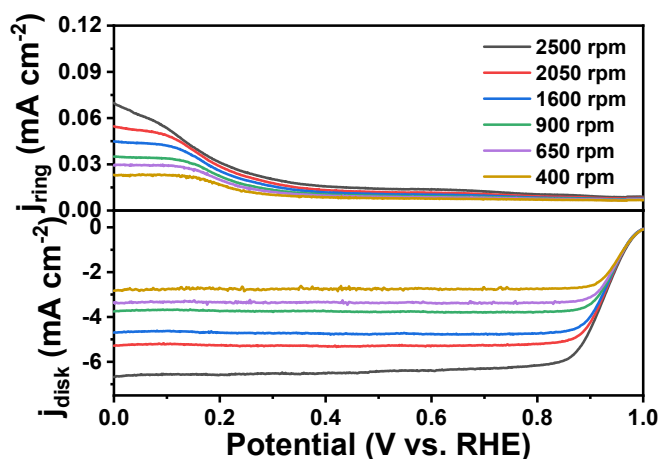


Fig. S10. Testing of the rotating disk electrode for Pt₂₃Pd₇₇ NSs/C catalysts.

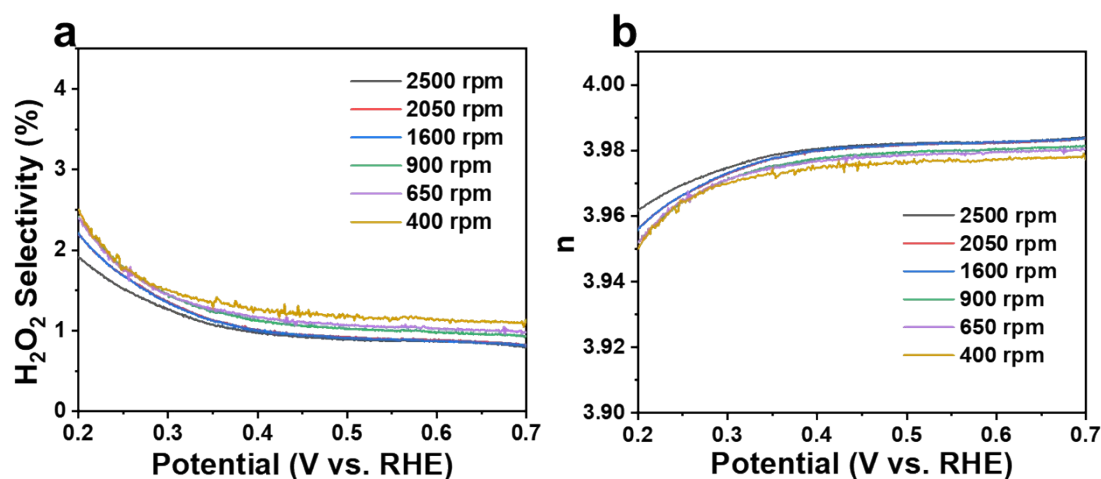


Fig. S11. (a) H₂O₂ selectivity and (b) electron transfer number of Pt₂₃Pd₇₇ NSs/C catalyst.

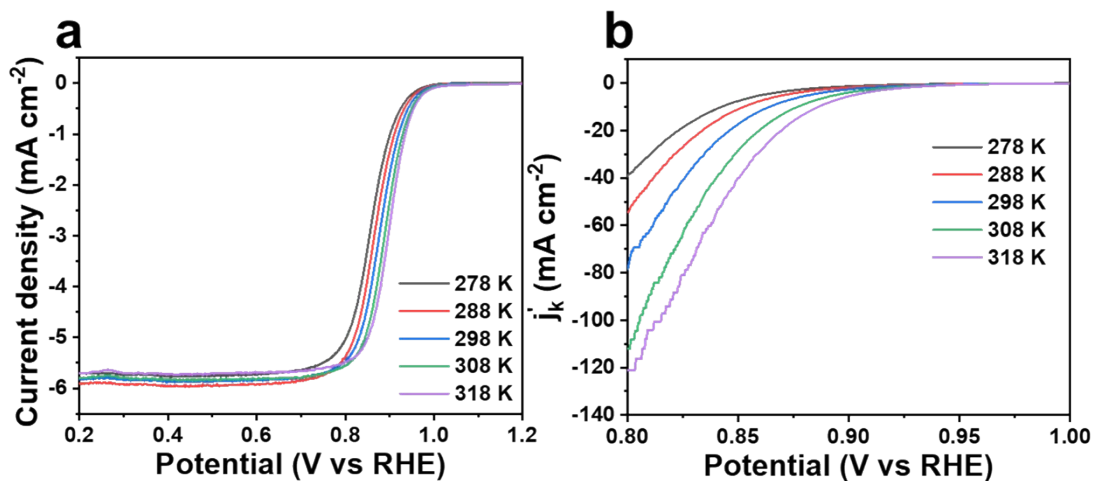


Fig. S12. (a) Polarization curve of Pt/C at different temperatures. (b) Kinetic current polarization curve of Pt/C at different temperatures.

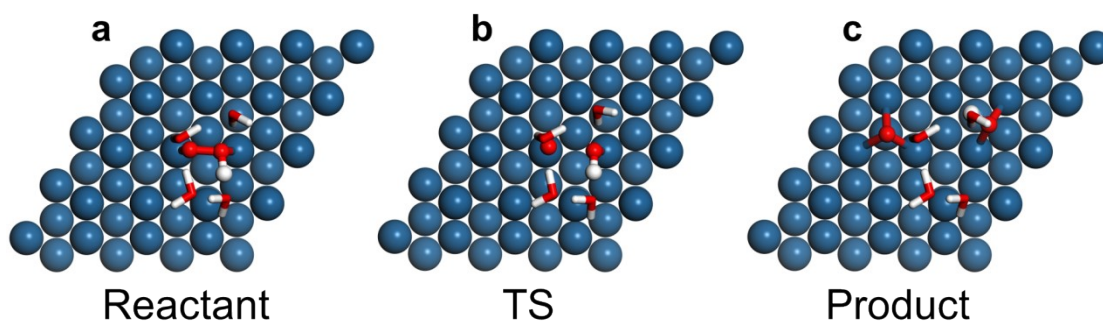


Fig. S13. The model of reactant(a), transition state(b) and product(c) during RDS.

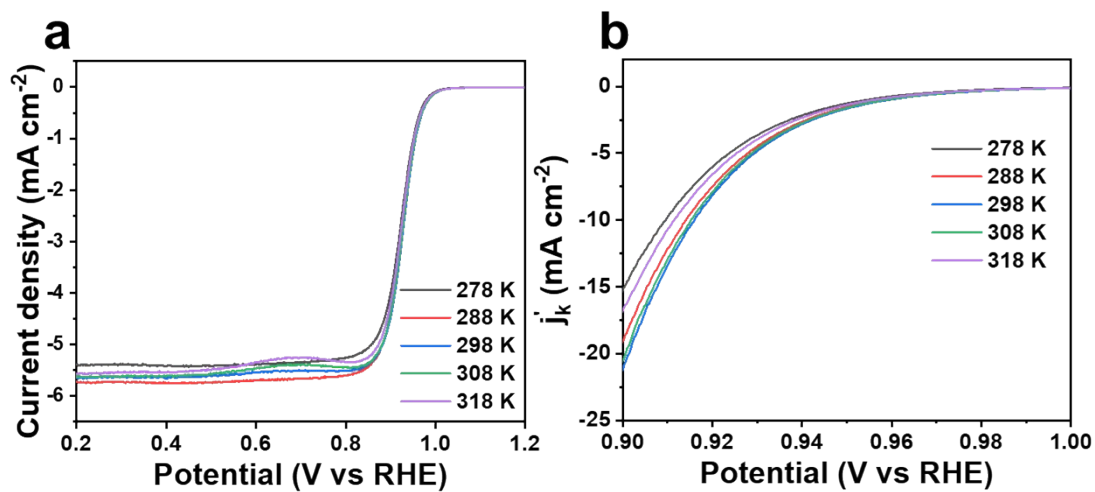


Fig. S14. (a) Polarization curve of Pt₂₃Pd₇₇ NSs at different temperatures. (b) Kinetic current polarization curve of Pt₂₃Pd₇₇ NSs at different temperatures.

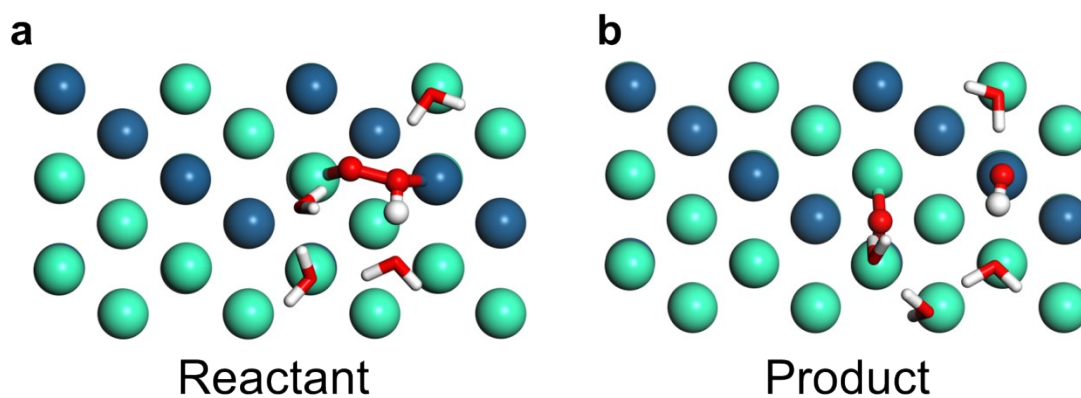


Fig. S15. The model of reactant(a) and product(b) during RDS.

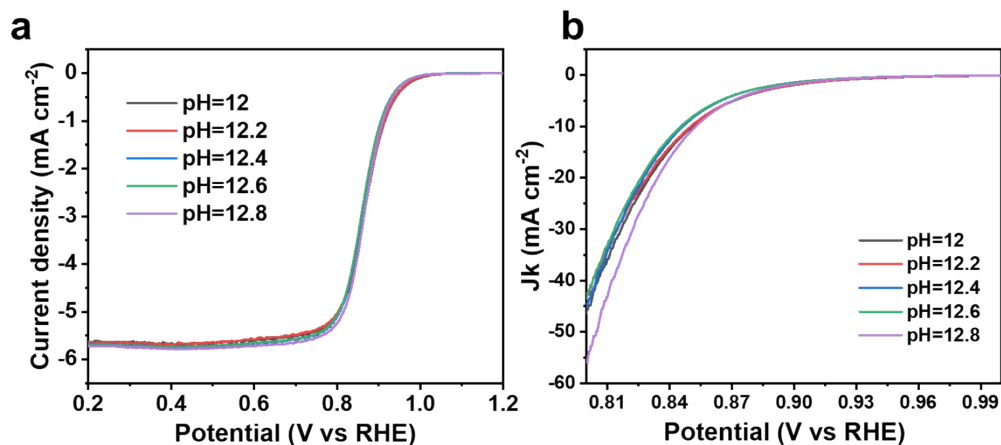


Fig. S16. (a) Polarization curves of Pt/C at different OH^- concentrations. (b) Kinetic current curves of Pt/C at different OH^- concentrations.

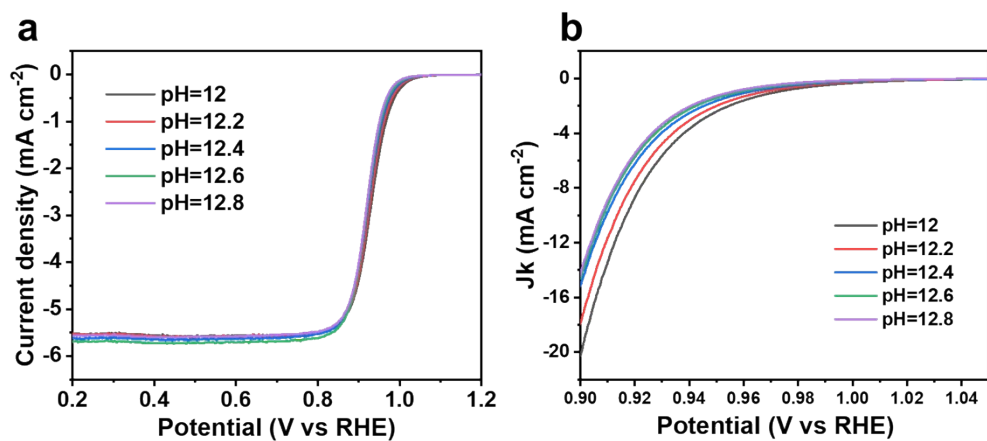


Fig. S17. (a) Polarization curves of $\text{Pt}_{23}\text{Pd}_{77}$ NSs at different OH^- concentrations. (b) Kinetic current curves of $\text{Pt}_{23}\text{Pd}_{77}$ NSs at different OH^- concentrations.

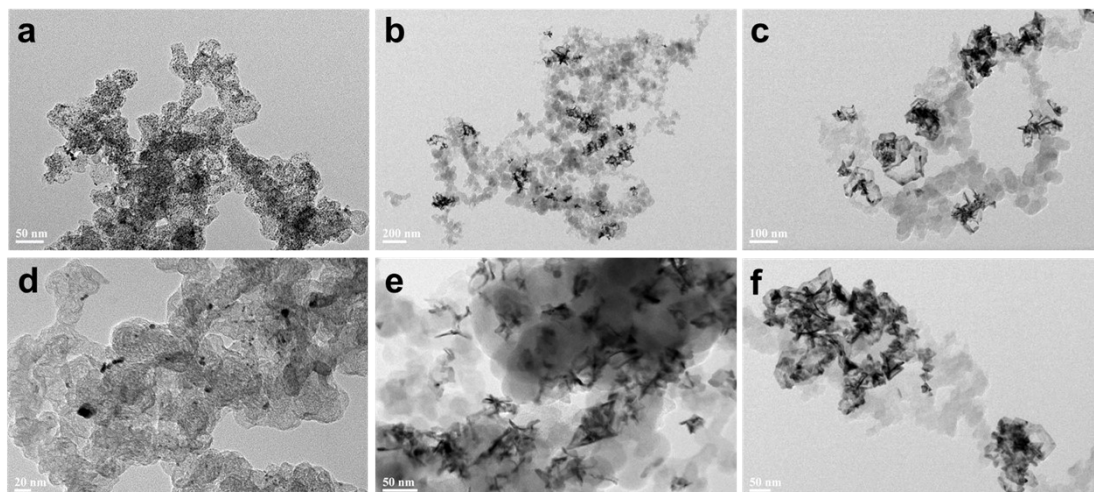


Fig. S18. Comparison of TEM images of (a, d) commercial Pt/C, (c, e) Pt₂₃Pd₇₇ NSs, and (d, f) Pd NSs before and after 10,000 cycles.

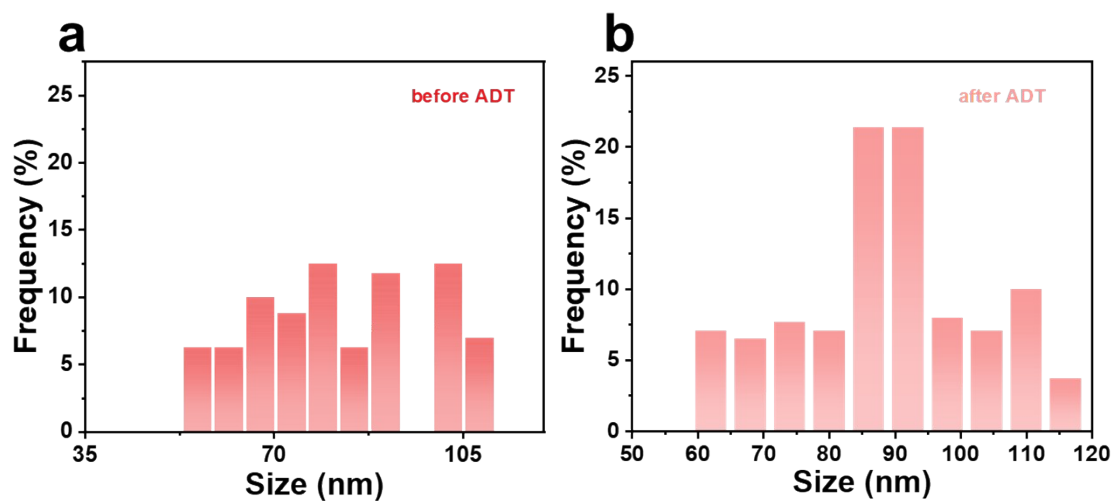


Fig. S19. Pt₂₃Pd₇₇ NSs/C catalyst size statistics before and after ADT. (a) before 10,000 cycles. (b) after 10,000 cycles.

Table S1 Comparison of ORR catalysis performance parameters (MA at 0.90 V_{RHE} E_{1/2} and Tafel slope) among representative Pt and Pd-based ORR catalysts in alkaline electrolytes

Catalysts	Mass activity at 0.9 V _{RHE} (A mg ⁻¹)	E _{1/2} (V _{RHE})	Tafel (mV dec ⁻¹)	Reference
Pt ₂₃ Pd ₇₇ NSs	6.78	0.946	40.06	This Work
Pd NSs	3.02	0.931	41.74	This Work
PdZn BMene	1.11	1.05	65.5	1
Pd metallene	0.43	1.0	74.7	1
c/a Pd@Pd NSs	1.78	0.932	51.3	2
PdMo bimetallene	16.37	0.95	*53	3
Pd NSs	8.02	*0.95	*60	4

Table S2 Apparent activation energy of Pt₂₃Pd₇₇/C catalyst.

Potential (V)	Slope	Ea (kJ mol ⁻¹)
0.84	-5367.13	44.62
0.85	-5498.40	45.71
0.86	-5593.62	46.50
0.87	-5544.47	46.10
0.88	-5407.16	44.96
0.89	-5228.81	43.47

Table S3 Apparent activation energy of Pt/C catalyst.

Potential (V)	Slope	Ea (kJ mol ⁻¹)
0.84	-5367.13	44.62
0.85	-5498.40	45.71
0.86	-5593.62	46.50
0.87	-5544.47	46.10
0.88	-5407.16	44.96
0.89	-5228.81	43.47

Reference

1. Zhang, H.; Li, X.; Wang, Y.; Deng, K.; Yu, H.; Xu, Y.; Wang, H.; Wang, Z.; Wang, L., Porous PdZn bimetallic for oxygen reduction electrolysis. *Applied Catalysis B: Environmental* **2023**, 338.
2. Lyu, Z.; Cai, J.; Zhang, X. G.; Li, H.; Huang, H.; Wang, S.; Li, T.; Wang, Q.; Xie, Z.; Xie, S., Biphasic Pd Nanosheets with Atomic-Hybrid RhOx/Pd Amorphous Skins Disentangle the Activity-Stability Trade-Off in Oxygen Reduction Reaction [J]. *Advanced Materials*. **2024**, 36 (24): 2314252.
3. Luo, M.; Zhao, Z.; Zhang, Y.; Sun, Y.; Xing, Y.; Lv, F.; Yang, Y.; Zhang, X.; Hwang, S.; Qin, Y.; Ma, J.-Y.; Lin, F.; Su, D.; Lu, G.; Guo, S., PdMo bimetallic for oxygen reduction catalysis. *Nature*. **2019**, 574 (7776), 81-85.
4. Lei Wang, Z. Z., Wenpei Gao, Tristan Maxson, David Raciti, Michael Giroux, Xiaoqing Pan, Chao Wang, Jeffrey Greeley, Tunable intrinsic strain in two-dimensional transition metal electrocatalysts. *Science*. **2019**, 363 (6429), 870-874.